Table S1 Atmospheric CO_2 measurement stations (data coverage > 15 years in the period of 1980-2012) used in the study and estimated trends of peak-to-trough amplitude (AMP_{P-T}) and trough-to-peak amplitude (AMP_{T-P}). The 95% confidence intervals were calculated for each trend estimate.

Station name	abbreviation	Latitude (°N)	Longitude (°E)	Period	AMP_{P-T} (ppm yr^{-1})	AMP_{T-P} (ppm yr^{-1})
Alert, Nunavut	ALT	82.45	-62.52	1985-2012	0.100 ±0.036	-0.096 ±0.042
Ny-Alesund, Svalbard	ZEP	78.91	11.89	1994-2012	0.128 ±0.056	-0.130 ±0.076
Mould Bay, Northwest Territories	MBC	76.25	-119.35	1980-1997	0.097 ±0.090	-0.141 ±0.098
Summit	SUM	72.60	-38.42	1997-2012	0.148 ±0.111	-0.160 ±0.117
Barrow, Alaska	BRW	71.32	-156.60	1980-2012	0.097 ±0.032	-0.090 ±0.033
Ocean Station M	STM	66.00	2.00	1981-2009	0.055 ±0.024	-0.056 ±0.027
Storhofdi, Vestmannaeyjar	ICE	63.40	-20.29	1992-2012	0.055 ±0.053	-0.053 ±0.066
Baltic Sea	BAL	55.50	16.67	1992-2011	-0.025 ±0.323	0.063 ±0.319
Cold Bay, Alaska	CBA	55.20	-162.72	1980-2012	0.071 ±0.042	-0.069 ±0.043
Mace Head, County Galway	MHD	53.33	-9.90	1991-2012	0.025 ±0.076	-0.042 ±0.100
Shemya Island, Alaska	SHM	52.72	174.10	1985-2012	0.049 ±0.071	-0.036 ±0.070
Hegyhatsal	HUN	46.95	16.65	1993-2012	0.011 ±0.542	-0.055 ±0.573
Cape Meares, Oregon	CMO	45.48	-123.97	1982-1997	-0.036 ±0.190	0.045 ±0.205

Ulaan Uul	UUM	44.45	111.10	1992-2012	-0.145 ±0.141	0.079 ±0.136
Niwot Ridge, Colorado	NWR	40.05	-105.63	1980-2012	-0.010 ±0.046	0.006 ±0.045
Wendover, Utah	UTA	39.90	-113.72	1993-2012	0.047 ±0.143	-0.070 ±0.161
Terceira Island, Azores	AZR	38.75	-27.08	1980-2012	0.014 ±0.066	-0.003 ±0.045
Tae-ahn Peninsula	TAP	36.73	126.13	1990-2012	0.008 ±0.305	-0.013 ±0.272
Mt. Waliguan	WLG	36.27	100.92	1990-2012	0.015 ±0.106	0.003 ±0.116
St. Davids Head, Bermuda	BME	32.37	-64.65	1989-2010	0.088 ±0.123	-0.108 ±0.141
Tudor Hill, Bermuda	BMW	32.26	-64.88	1989-2012	-0.002 ±0.097	-0.022 ±0.102
WIS Station, Negev Desert	WIS	30.86	34.78	1995-2012	0.035 ±0.126	-0.026 ±0.173
Izana, Tenerife, Canary Islands	IZO	28.30	-16.48	1991-2012	0.014 ±0.049	-0.018 ±0.058
Sand Island, Midway	MID	28.22	-177.37	1985-2012	0.060 ±0.051	-0.062 ±0.055
Key Biscayne, Florida	KEY	25.67	-80.20	1980-2012	0.010 ±0.040	-0.012 ±0.039
Assekrem	ASK	23.26	5.63	1995-2012	0.022 ±0.038	-0.027 ±0.048

Table S2 Details of dynamic global vegetation models used in this study. Among the nine models, eight models (CLM4.5, ISAM, JULES, LPJ, LPX, OCN, ORCHIDEE and VISIT) are from the TRENDY project and performed three simulations (S1, S2 and S3) following the TRENDYv2 protocol. In simulation S1, only atmospheric CO_2 concentration was varied. In simulation S2, atmospheric CO_2 and climate were varied. In simulation S3, atmospheric CO_2, climate and land use were varied. Note that models differ in the representation of land use change processes (Table S3).

Model Name	Abbreviation	Spatial Resolution	Period	Reference
Community Land Model version 4.5	CLM4.5	1.25 °×0.9375 °	1860-2012	Oleson *et al.*, 2013
Integrated Science Assessment Model	ISAM	0.5 °× 0.5 °	1901-2012	Jain *et al.*, 2013
The Joint UK Land Environment Simulator	JULES	1.875 °×1.25 °	1860-2012	Clark *et al.*, 2011
Lund-Potsdam-Jena	LPJ	0.5 °× 0.5 °	1901-2012	Sitch *et al.*, 2003
Land Surface Processes and Exchanges	LPX	1 °× 1 °	1860-2012	Stocker *et al.*, 2013
ORCHIDEE-CN	OCN	1 °× 1 °	1901-2012	Zaehle & Friend, 2010
Organizing Carbon and Hydrology in Dynamic Ecosystems	ORCHIDEE	2 °× 2 °	1901-2012	Krinner *et al.*, 2005
Vegetation Integrative Simulator for Trace gases	VISIT	0.5 °× 0.5 °	1901-2012	Kato *et al.*, 2013
Community Land Model version 4.0	CLM4	0.5 °× 0.5 °	1850-2012	Oleson *et al.*, 2010; Mao *et al.*, 2013

Table S3 Processes of land use change and management considered in TRENDYv2 models (Le Quéré *et al.*, 2014).

	CLM4.5	ISAM	JULES	LPJ	LPX	OCN	ORCHIDEE	VISIT
Deforestation and forest regrowth after abandonment	√	√	√	√	√	√	√	√
Wood harvest and forest degradation	√	√						√
Shifting cultivation	√							√
Cropland harvest	√				√	√	√	√
Peat fires	√							
Fire simulation and/or suppression	√			√	√			√

Table S4 Summary of transport simulations performed. We use 9 dynamic global vegetation models (see Table S2) to simulate land-atmosphere CO_2 exchange (NEE), 1 model to simulate ocean-atmosphere CO_2 exchange and gridded monthly fossil fuel CO_2 emission from CDIAC. Then LMDZ4, a 3D atmospheric tracer transport model, is performed to transport carbon flux into a point estimate of CO_2 concentration at each observation station. The land-atmosphere CO_2 exchange is varying in transport simulations T1~T5 but constant at 1979 value in T6~T8. Among these eight transport simulations, T1 indicates the effect of all factors, while T6 indicates the effect of wind. The effects of CO_2 fertilization, climate change, land use change, nitrogen deposition, fossil fuel and ocean flux are estimated from (T2-T6), (T3-T2), (T4-T3), T5, (T7-T6) and (T8-T6), respectively. Note that in transport simulations T1~T4 and T6~T8, land-atmosphere CO_2 exchange was derived from eight TRENDYv2 models; in transport simulation T5, land-atmosphere CO_2 exchange was derived from CLM4 model only (Table S2).

Transport Simulation	**Land-atmosphere CO_2 exchange**				**Fossil fuel**	**Ocean-atmosphere CO_2 exchange**	**Wind**
	CO_2	**Climate**		**Nitrogen deposition**			
T1	vary	vary	vary	-	vary	vary	vary
T2	vary	constant	constant	-	constant	constant	vary
T3	vary	vary	constant	-	constant	constant	vary
T4	vary	vary	vary	-	constant	constant	vary
T5	constant	constant	constant	vary	constant	constant	constant
T6	constant	constant	constant	-	constant	constant	vary
T7	constant	constant	constant	-	vary	constant	vary
T8	constant	constant	constant	-	constant	vary	vary

Figure S1 Spatial distribution of the NOAA-ERSL stations (data coverage > 15 years) used in this study. Stations in northern temperate region (23-50 ℃N) and boreal region (north of 50 ℃N) are shown in red and blue, respectively. Station abbreviations are defined in Table S1.

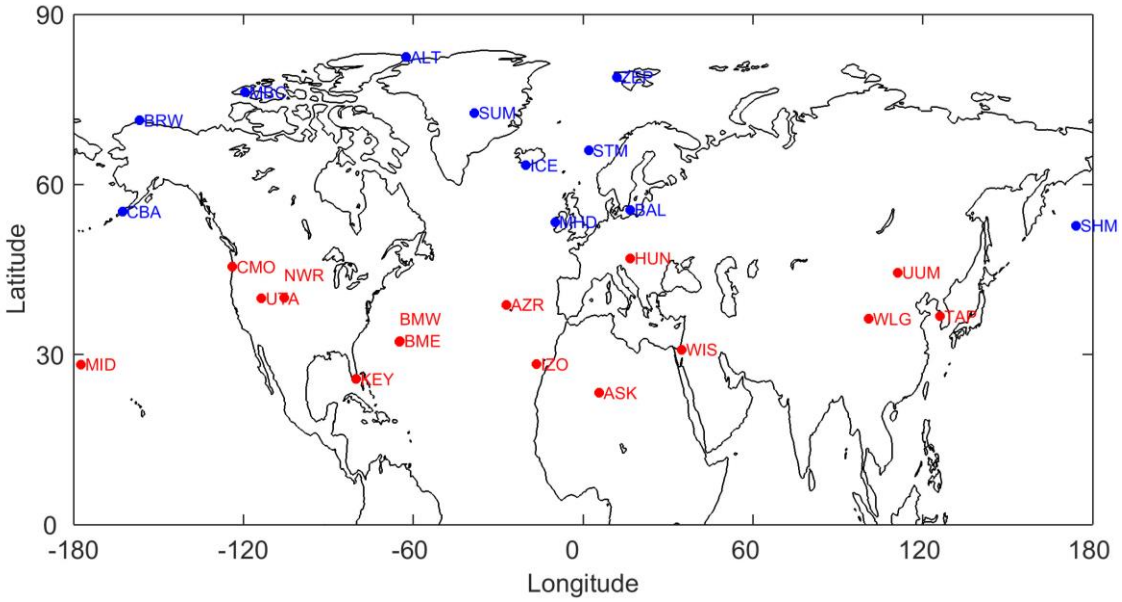

Figure S2 A schematic describing the terms we used to characterize the seasonal amplitude of atmospheric CO_2. In this example, we show the detrended seasonal cycle of CO_2 at Barrow, Alaska (BRW, 71°N) during 1980-1981. The peak (maximum) value and the trough (minimum) value of CO_2 cycle in each year are marked in blue and red circle, respectively. We divided CO_2 amplitude into peak-to-trough (AMP_{P-T}) and trough-to-peak (AMP_{T-P}). AMP_{P-T} was calculated as the difference between the peak value and the trough value of CO_2 seasonal cycle in a year (blue line), while AMP_{T-P} was calculated as the difference between the trough value of CO_2 seasonal cycle in a year and the peak value of the cycle in the next year (red line). The AMP_{P-T} and AMP_{T-P} represent seasonal variation in atmospheric CO_2 concentration during the net carbon uptake period (marked in light gray) and the net carbon release period (marked in dark gray), respectively. Note that the sign convention is positive for AMP_{P-T} and negative for AMP_{T-P}.

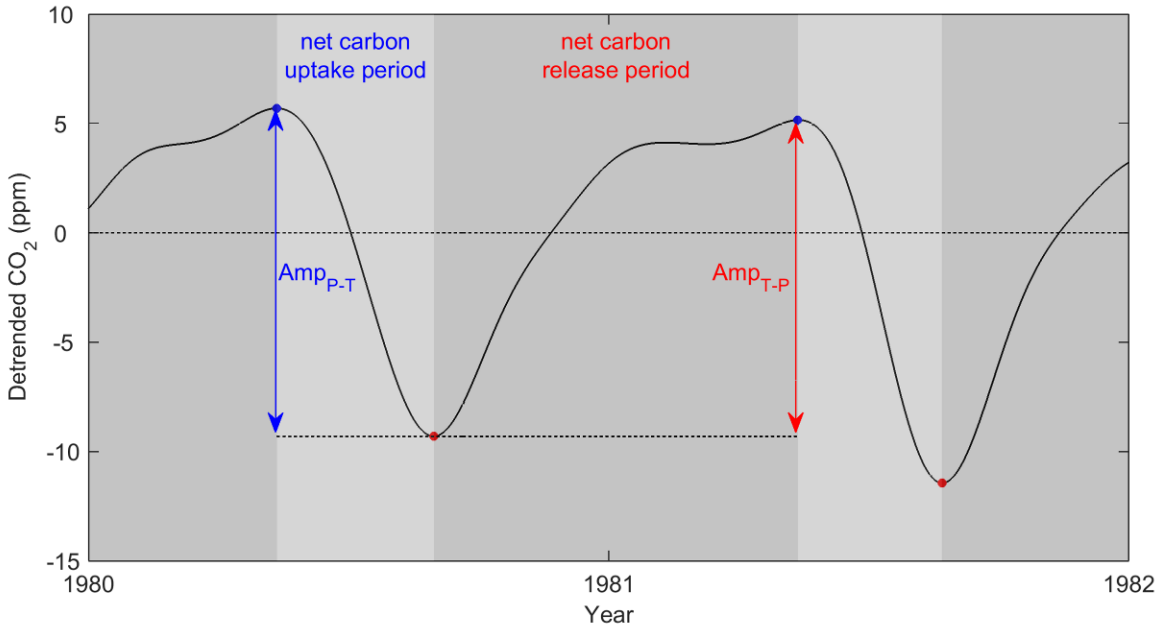

Figure S3 Observed trends in monthly net CO_2 concentration change (MNCC) from long-term records of the global NOAA-ERSL surface flask air-sampling network. Here the monthly net CO_2 concentration change (MNCC) was calculated as the difference between the detrended CO_2 value in the first week of a given month and that of next month. Shown on the top of the figure are the abbreviated names of 26 atmospheric CO_2 concentration measurement stations in northern temperate and boreal regions. We sort the stations according to their latitudes, from 23 ℕ to 90 ℕ. Each row represents trends in MNCC for a certain month at different stations, while each column represents trends in MNCC for different months at a certain station. Gray grids show insignificant trends ($P > 0.10$), while colored grids without slashes indicate statistically significant ($P < 0.05$) and those with slashes marginal significant ($P < 0.10$). The number in each grid shows the value of the trend. Station abbreviations are defined in Table S1.

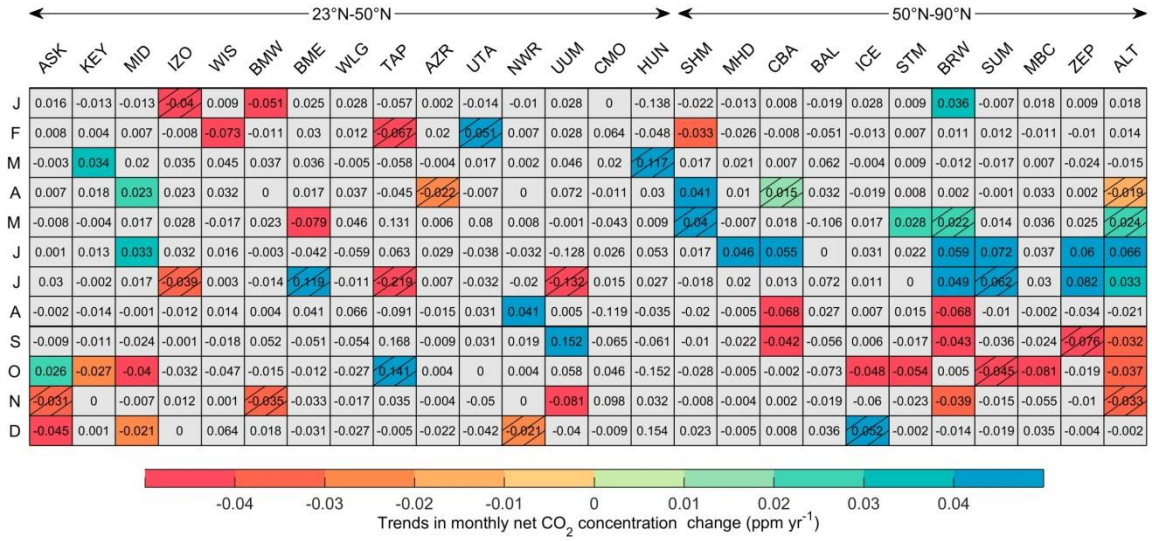

Figure S4 Observed and modeled trends in CO_2 seasonal peak-to-trough amplitude (AMP_{P-T}) (a, c) and trough-to-peak amplitude (AMP_{T-P}) (b, d) during 1980 to 2012, averaged over the stations from northern temperate region (23-50ºN) and boreal region (north of 50ºN). In (a) and (b), all stations in northern temperate and boreal region are included. In (c) and (d), only stations with observed significant AMP trends are taken into account. Here the modeled trends were calculated based on eight TRENDY models under T1 transport simulation (see methods). We also calculated the multi-model ensemble mean (MMEM) trends. Uncertainties are shown by error bars based on the standard deviation of AMP trends across stations in each region.

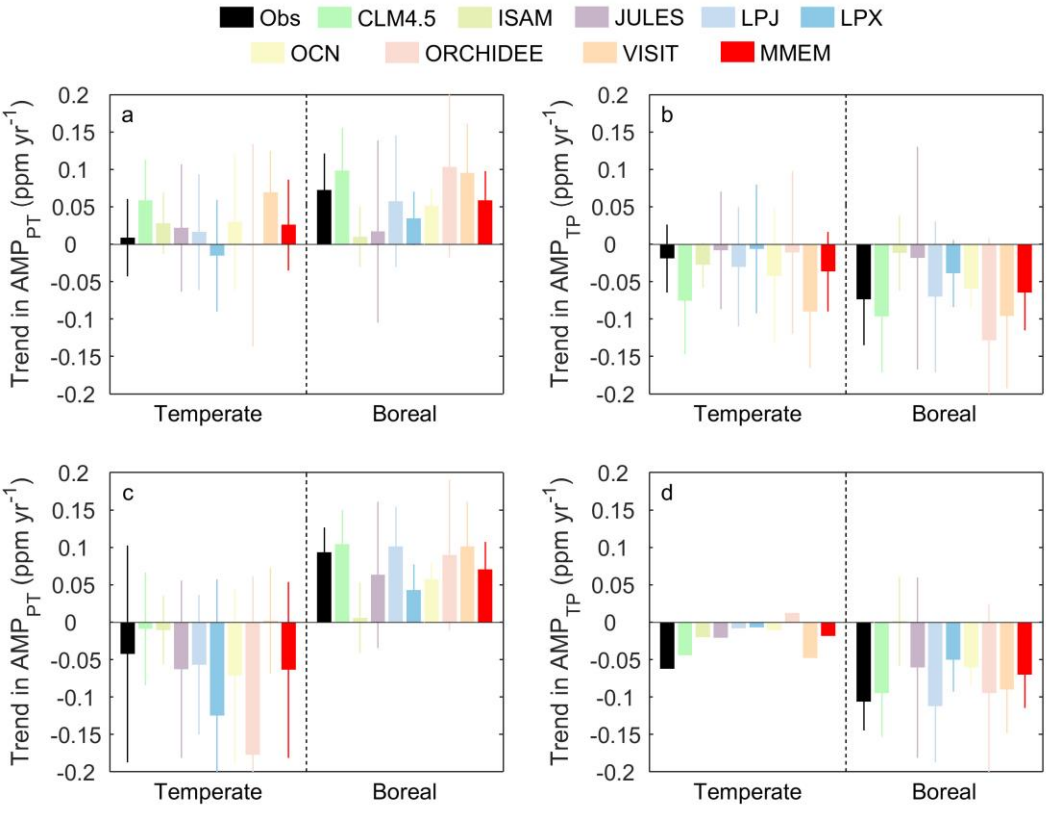

Figure S5 Spatial distribution of trends in temperature (a) and precipitation (b) from April to August during the period 1980-2012. Note that the period from April to August corresponds to the carbon uptake period of most northern temperate and boreal stations. Regions with mean annual NDVI (AVHRR NDVI3 g dataset) less than 0.1 were masked.

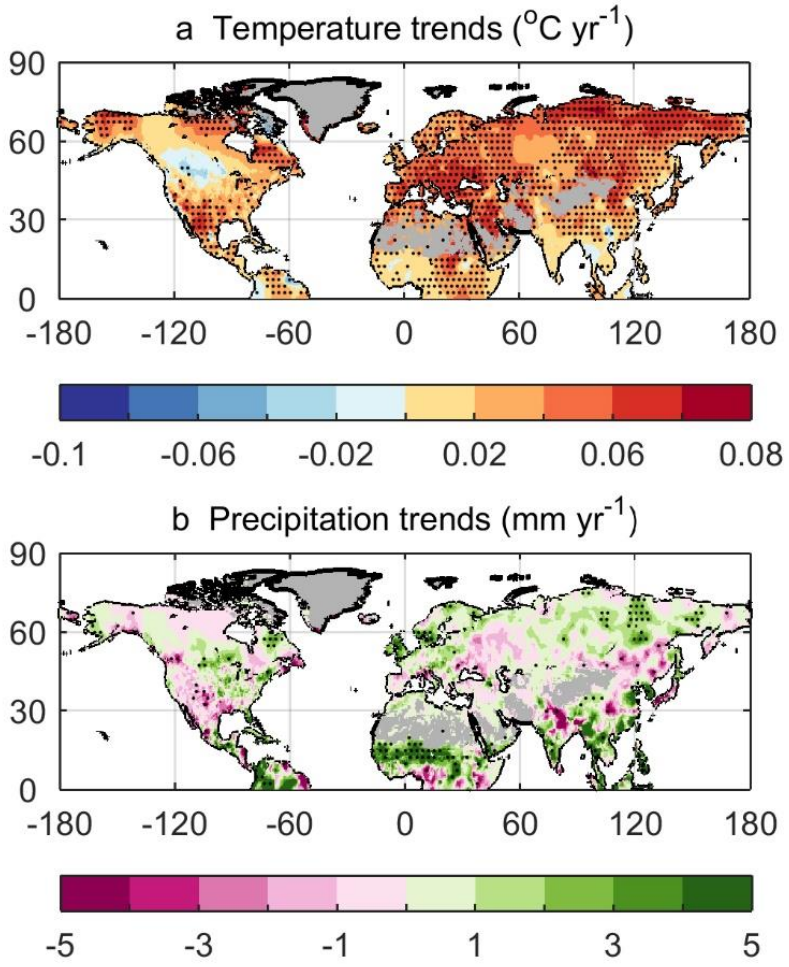

Figure S6 Trends in monthly net CO_2 concentration change (MNCC) estimated by process-based models at Barrow, Alaska (BRW) during carbon uptake period (CUP) (a) and those during carbon release period (CRP) (b) from 1980 to 2012. Model scenario simulations include change in atmospheric CO_2 ('CO_2'), climate ('CLIM'), land use ('LU'), fossil fuel ('FF'), ocean-air carbon flux ('Ocean'), wind ('Wind') and nitrogen deposition ('NDEP'). For a certain scenario simulation (except "NDEP"), the different colored bars show the trends in MNCC of different months derived from multi-model ensemble mean (MMEM). For 'NDEP' scenario, the different colored bars show results from CLM4 model only. The vertical solid lines indicate the maximum and minimum trends across models. We also calculated the total monthly trends during CUP (CRP) and denote them with horizontal black solid lines. Note that the carbon uptake period (CUP) at BRW station refers to the period from May to August during which positive values of MNCC are detected. Similarly, carbon release period (CRP) refers to the period from September to April during which negative values of MNCC are obtained.

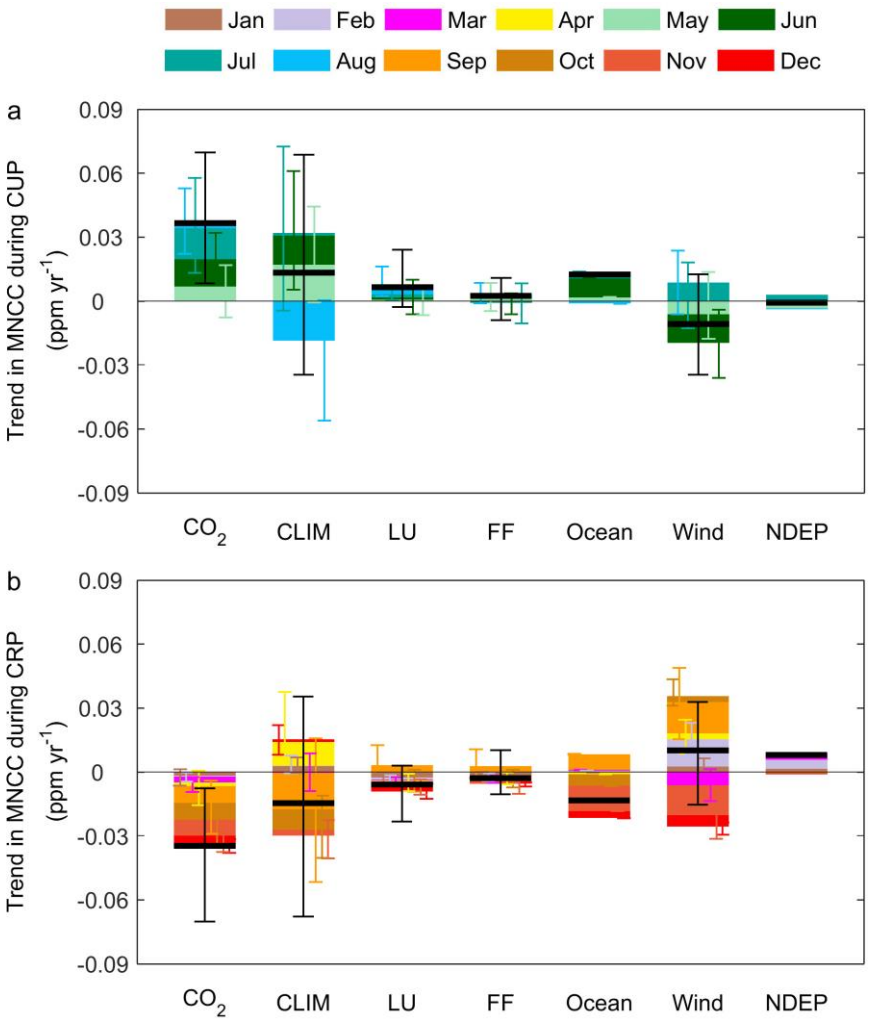

Figure S7 Spatial distribution of trends in net biome productivity (NBP) obtained from eight TRENDY models driven by rising CO_2 (a), climate change (b) and land use change (c) from April to August. Note that the period from April to August corresponds to the carbon uptake period of most northern temperate and boreal stations. Regions with mean annual NDVI (AVHRR NDVI3 g dataset) less than 0.1 were masked. The study period is from 1980 to 2012.

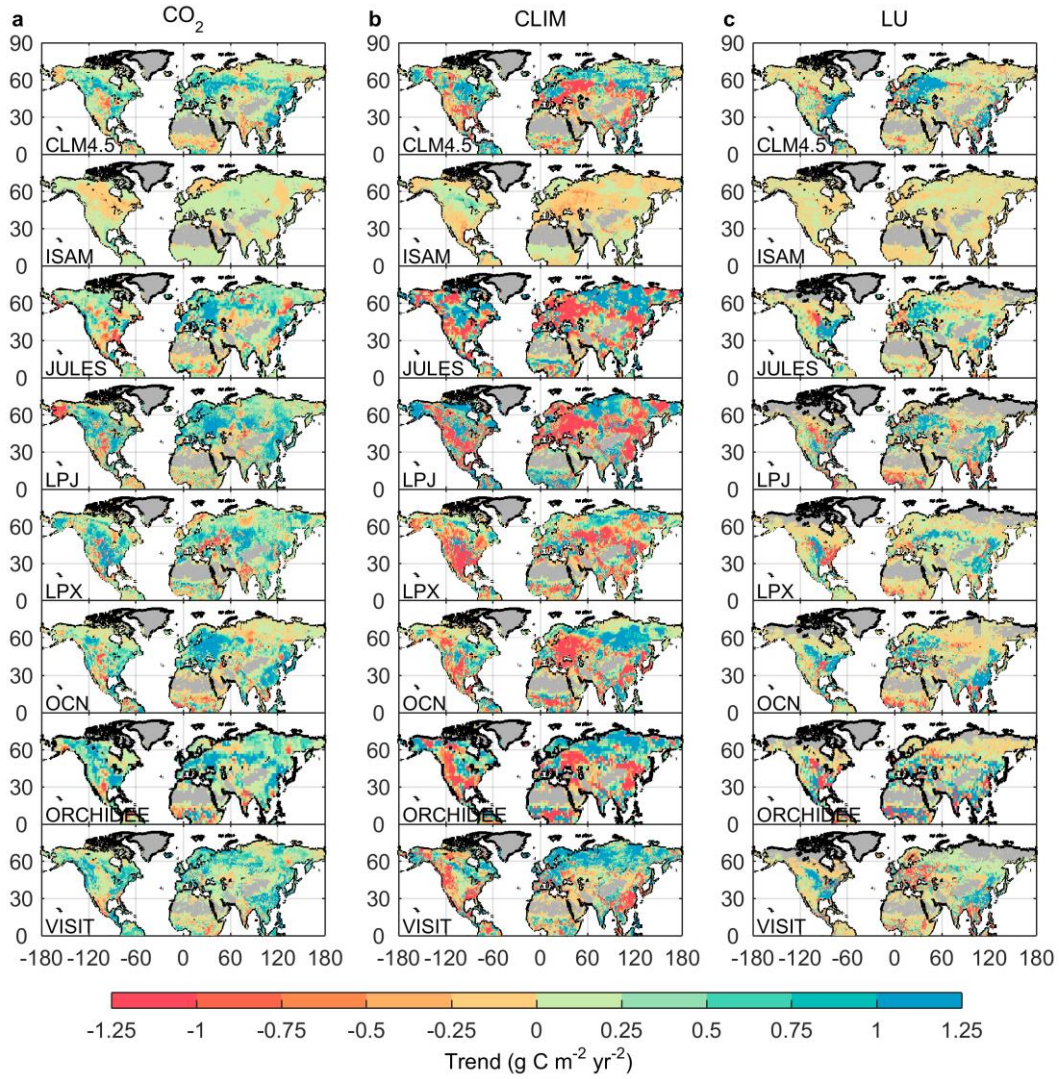

Figure S8 Trends in CO_2 seasonal peak-to-trough amplitude (AMP_{P-T}) estimated by eight TRENDY models and multi-model ensemble mean (MMEM) under different scenario simulations at northern temperate and boreal stations. The scenario simulations include 'CO_2' (a), 'CLIM' (b), 'LU' (c), 'Fossil fuel' (d), 'Ocean' (e) and 'Wind' (f) (Table S4). Gray grids show insignificant trends (P > 0.10), while colored grids without slashes indicate statistically significant (P < 0.05) and those with slashes marginal significant (P < 0.10). The number in each grid shows the value of the trend. Station abbreviations are defined in Table S1.

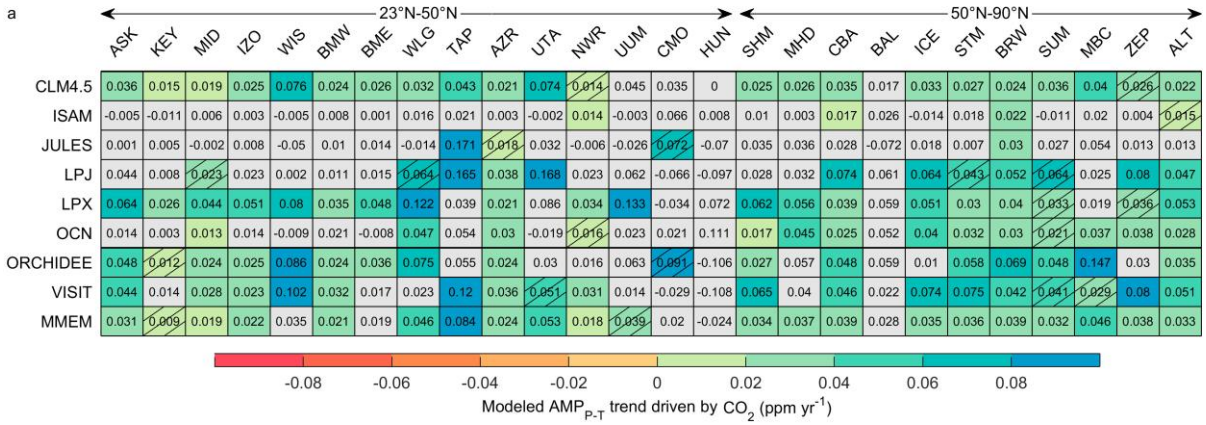

d

	23°N-50°N														50°N-90°N										
	ASK	KEY	MID	IZO	WIS	BMW	BME	WLG	TAP	AZR	UTA	NWR	UUM	CMO	HUN	SHM	MHD	CBA	BAL	ICE	STM	BRW	SUM	MBC	ZEP	ALT
CLM4.5	-0.005	-0.015	-0.005	-0.008	0.01	-0.002	-0.025	0.001	-0.01	0.005	0.005	0.006	-0.001	-0.014	-0.079	-0.014	-0.007	0.007	0.009	-0.001	0.007	-0.002	-0.009	-0.006	-0.002	0
ISAM	0.003	-0.01	-0.001	-0.006	-0.012	0.002	-0.003	-0.008	-0.062	0	-0.019	0.006	-0.017	0.023	-0.059	-0.007	-0.024	-0.012	0.022	-0.004	0.003	-0.021	0.012	0.008	0.013	0.002
JULES	0.003	-0.022	-0.012	-0.001	-0.043	0.012	-0.044	-0.02	-0.019	0.027	-0.022	-0.006	-0.039	-0.012	-0.083	0.027	0.024	0.002	0.015	0.031	0	-0.011	0.009	-0.056	0.03	0.012
LPJ	-0.01	-0.036	0	-0.006	-0.02	-0.014	-0.022	-0.036	0.022	0.007	-0.146	-0.016	-0.033	-0.02	-0.14	-0.017	-0.009	0.045	0.019	0.023	0.004	0.012	-0.006	-0.038	0.027	0.006
LPX	0.018	-0.001	0.002	0.005	-0.011	0.001	-0.01	-0.019	-0.006	0.002	-0.005	-0.003	0.06	-0.057	-0.078	0.002	-0.005	0.003	-0.005	0.005	0.003	0.008	-0.001	0.01	-0.006	0.002
OCN	0.002	-0.016	0	-0.016	0.035	-0.005	-0.017	0.004	-0.053	0.002	-0.041	-0.011	-0.026	0.009	0.005	0	-0.011	0	0.002	0.005	-0.006	0.004	0.001	0.007	0.017	-0.001
ORCHIDEE	0.009	0.017	0.002	0.007	-0.006	0.001	0.008	0.004	0.016	-0.005	-0.063	-0.009	-0.008	-0.03	-0.13	0	-0.01	0.007	0.064	-0.002	0.009	0.012	0.005	0.002	0.023	0.01
VISIT	0.006	-0.016	0.009	0.006	0.019	-0.018	0.015	0.025	0.028	0.001	-0.028	0.007	0.009	-0.025	-0.096	0.023	-0.021	0.004	-0.006	0.026	-0.005	-0.002	-0.003	0.009	-0.001	-0.004
MMEM	0.003	-0.013	-0.001	-0.002	-0.004	-0.003	-0.012	-0.006	-0.011	0.005	-0.04	-0.003	-0.007	-0.016	-0.082	0.002	-0.008	0.007	0.015	0.01	0.002	0	0.001	-0.008	0.013	0.003

Modeled AMP_{P-T} trend driven by Fossil fuel (ppm yr^{-1})

e

	23°N-50°N														50°N-90°N										
	ASK	KEY	MID	IZO	WIS	BMW	BME	WLG	TAP	AZR	UTA	NWR	UUM	CMO	HUN	SHM	MHD	CBA	BAL	ICE	STM	BRW	SUM	MBC	ZEP	ALT
CLM4.5	-0.002	-0.001	0.002	0	0.008	-0.002	0	0.003	0	-0.002	0.004	0	0.004	0.018	-0.003	-0.006	-0.001	-0.006	-0.004	0.01	0.005	0.01	-0.008	0.015	0.001	0.002
ISAM	-0.002	-0.001	0.003	0	0.007	-0.001	0	0.003	-0.001	-0.002	0.005	0	0.004	0.019	-0.003	-0.005	-0.001	-0.006	-0.005	0.007	0.005	0.01	-0.008	0.015	0.001	0.002
JULES	-0.002	-0.001	0.002	0	0.007	-0.002	0	0.003	0	-0.003	0.005	0	0.003	0.019	-0.003	-0.006	-0.001	-0.007	-0.004	0.008	0.005	0.01	-0.006	0.016	0.001	0.002
LPJ	-0.002	-0.001	0.003	0	0.008	-0.002	0	0.003	0	-0.002	0.004	0	0.004	0.018	-0.003	-0.005	-0.001	-0.006	-0.005	0.008	0.005	0.01	-0.007	0.014	0.002	0.002
LPX	-0.002	-0.001	0.003	0	0.007	-0.002	0	0.003	-0.001	-0.003	0.004	0	0.004	0.02	-0.003	-0.006	0	-0.006	-0.005	0.01	0.005	0.01	-0.008	0.015	0.001	0.002
OCN	-0.002	-0.001	0.003	0	0.007	-0.002	-0.001	0.003	-0.001	-0.003	0.004	0	0.004	0.019	-0.003	-0.006	-0.001	-0.006	-0.006	0.009	0.005	0.01	-0.008	0.015	0	0.002
ORCHIDEE	-0.002	-0.001	0.003	0	0.007	-0.002	0	0.003	-0.001	-0.003	0.005	0	0.004	0.017	-0.003	-0.006	-0.001	-0.006	-0.005	0.008	0.005	0.01	-0.008	0.015	0.002	0.002
VISIT	-0.001	-0.001	0.003	0	0.007	-0.002	-0.001	0.003	0	-0.003	0.004	0	0.004	0.019	-0.003	-0.004	-0.001	-0.006	-0.005	0.008	0.005	0.01	-0.008	0.015	0.002	0.002
MMEM	-0.002	-0.001	0.003	0	0.007	-0.002	0	0.003	0	-0.003	0.004	0	0.004	0.019	-0.003	-0.005	-0.001	-0.006	-0.005	0.008	0.005	0.01	-0.008	0.015	0.001	0.002

Modeled AMP_{P-T} trend driven by Ocean (ppm yr^{-1})

f

	23°N-50°N														50°N-90°N										
	ASK	KEY	MID	IZO	WIS	BMW	BME	WLG	TAP	AZR	UTA	NWR	UUM	CMO	HUN	SHM	MHD	CBA	BAL	ICE	STM	BRW	SUM	MBC	ZEP	ALT
CLM4.5	0.028	0.016	-0.003	0.043	0.031	-0.033	0.042	0.018	-0.051	-0.014	0.031	-0.01	-0.181	-0.001	0.009	-0.017	-0.059	0.028	-0.015	0.033	0	0.027	0.036	0.121	-0.039	-0.01
ISAM	0.015	0.027	0.015	0.043	0.066	0.011	0.064	0.015	0.04	-0.013	0.04	-0.021	-0.038	0.013	0.159	0.018	0.028	0.036	-0.027	0.024	-0.029	0.031	-0.021	0.073	-0.051	-0.014
JULES	-0.052	0.039	0.024	0.046	0.115	0.033	0.086	0.021	0.042	-0.039	0.022	-0.026	0.008	0.018	0.229	0.036	0.01	-0.019	-0.041	0.046	-0.018	0.008	-0.008	0.122	-0.057	-0.026
LPJ	-0.025	0.008	-0.001	0.029	0.063	-0.045	0.058	0.084	0.004	0.02	0.088	0.026	-0.085	-0.019	0.082	-0.062	-0.001	0.064	-0.097	0.007	0.015	0.024	0.056	0.038	-0.017	-0.011
LPX	0.027	-0.004	-0.009	0.02	-0.039	-0.016	-0.02	-0.017	-0.011	0.017	0.045	0.005	-0.205	0.027	-0.012	-0.035	0.016	0.002	0.005	0.008	-0.009	0.004	0.027	0.025	-0.002	0.001
OCN	-0.039	0.003	-0.023	0.023	-0.022	-0.03	-0.03	-0.005	0.121	0.02	0.044	0.001	-0.151	0.015	0.043	-0.022	0.004	0.016	0.015	0.017	-0.001	0	0.009	0.009	0	-0.008
ORCHIDEE	-0.03	-0.031	-0.055	0.015	-0.099	-0.088	-0.106	-0.101	0.047	0.067	0.061	0.028	-0.324	-0.114	0.159	-0.142	-0.002	-0.042	-0.086	0.029	-0.012	-0.008	0.023	-0.142	0.026	0
VISIT	0.047	0.034	-0.005	0.036	0.044	-0.036	0.024	0.078	0.021	-0.004	0.043	0.005	-0.114	0.113	-0.007	-0.026	-0.041	0.024	0.014	0.018	0.008	0.012	-0.003	0.054	0.009	-0.005
MMEM	-0.003	0.011	-0.007	0.032	0.02	-0.026	0.015	0.011	0.027	0.007	0.047	0.001	-0.136	0.007	0.083	-0.031	-0.006	0.014	-0.029	0.023	-0.006	0.012	0.015	0.037	-0.016	-0.009

Modeled AMP_{P-T} trend driven by Wind (ppm yr^{-1})

Figure S9 Same as Figure 2, but for trends in CO_2 seasonal trough-to-peak amplitude (AMP_{T-P}) (a) and trough-to-peak amplitude (AMP_{T-P}) (b) estimated by CLM4 model under nitrogen deposition scenarios at 26 northern temperate and boreal stations.

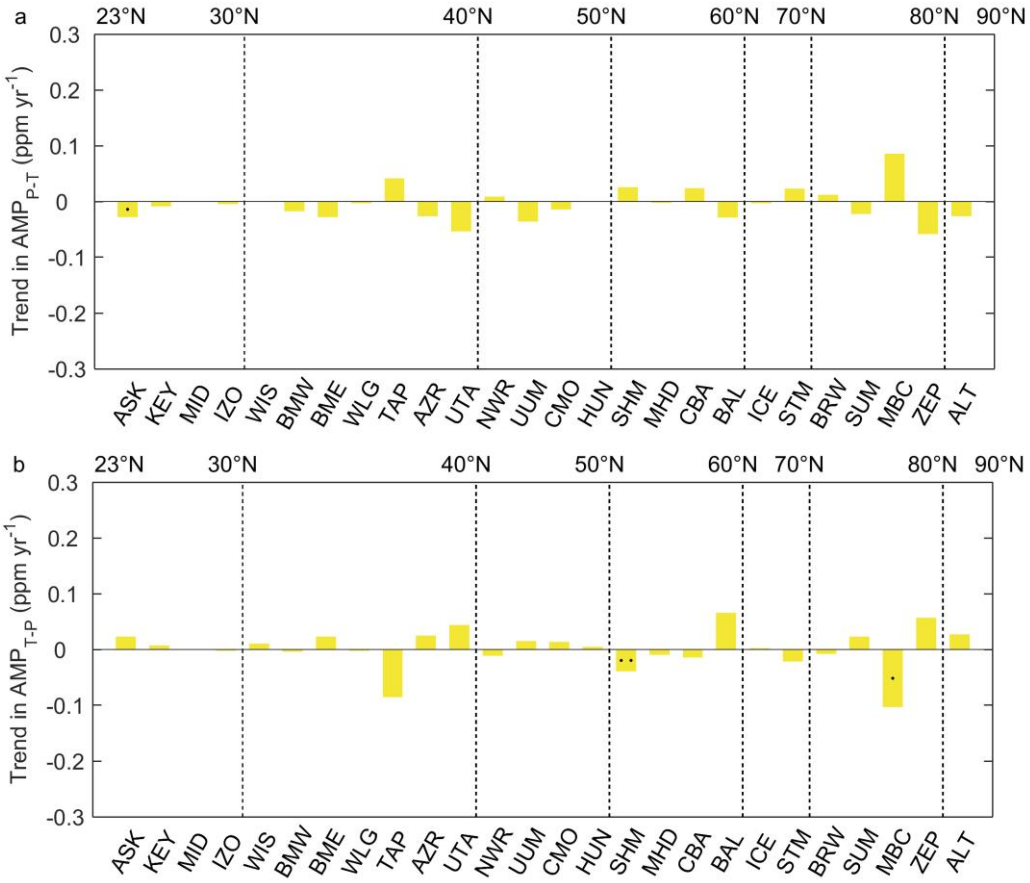

Figure S10 Trends in fossil fuel CO_2 emissions. (a) Time series of annual fossil fuel CO_2 emissions over global area, northern temperate area (23°N-50°N) and boreal area (north of 50°N) during 1980-2012. The slope of the trend and P values for different regions are denoted in different colors. (b) Spatial distribution of trends in fossil fuel CO_2 emissions from April to August. (c) Spatial distribution of trends in fossil fuel CO_2 emissions from September to March. Note that the months from April to August corresponds to the period calculating AMP_{P-T} for most northern temperate and boreal stations, while September to March corresponds to the period calculating AMP_{T-P}.

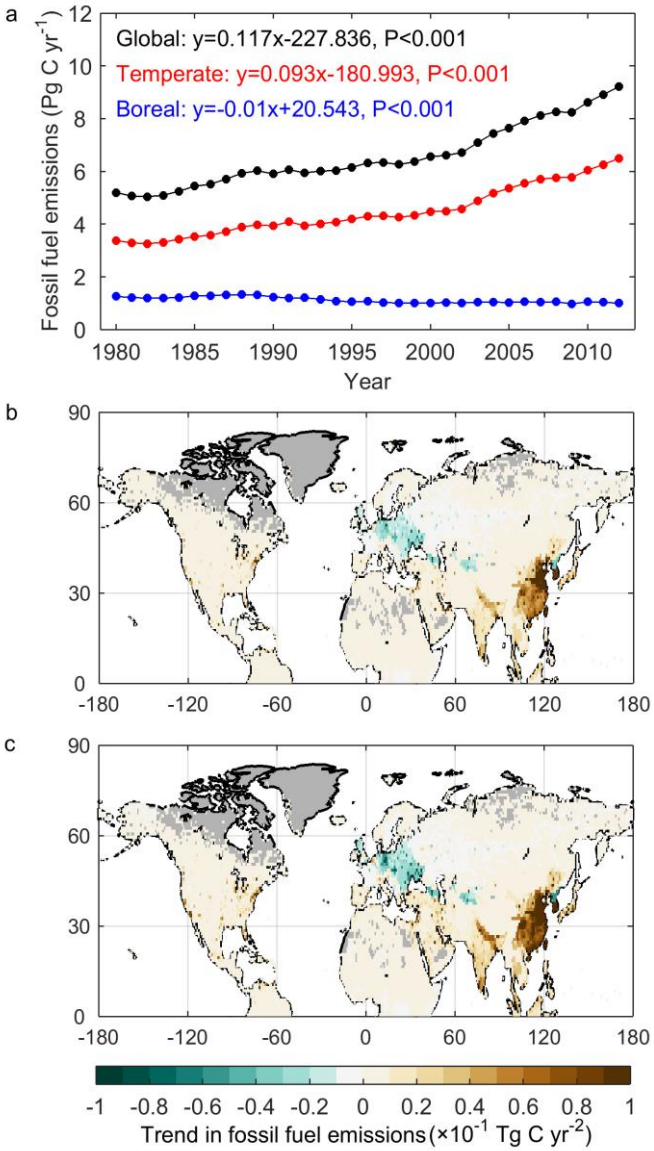

Figure S11 Spatial distribution of trends in net biome productivity (NBP) (a), gross primary productivity (GPP) (b) and total ecosystem respiration (TER) (c) from September to March for eight Trendy models driven by climate change only. Note that the period from September to March corresponds to the carbon release period (CRP) of most northern temperate and boreal stations. Regions with mean annual NDVI (AVHRR NDVI3 g dataset) less than 0.1 were masked. The study period is from 1980 to 2012.

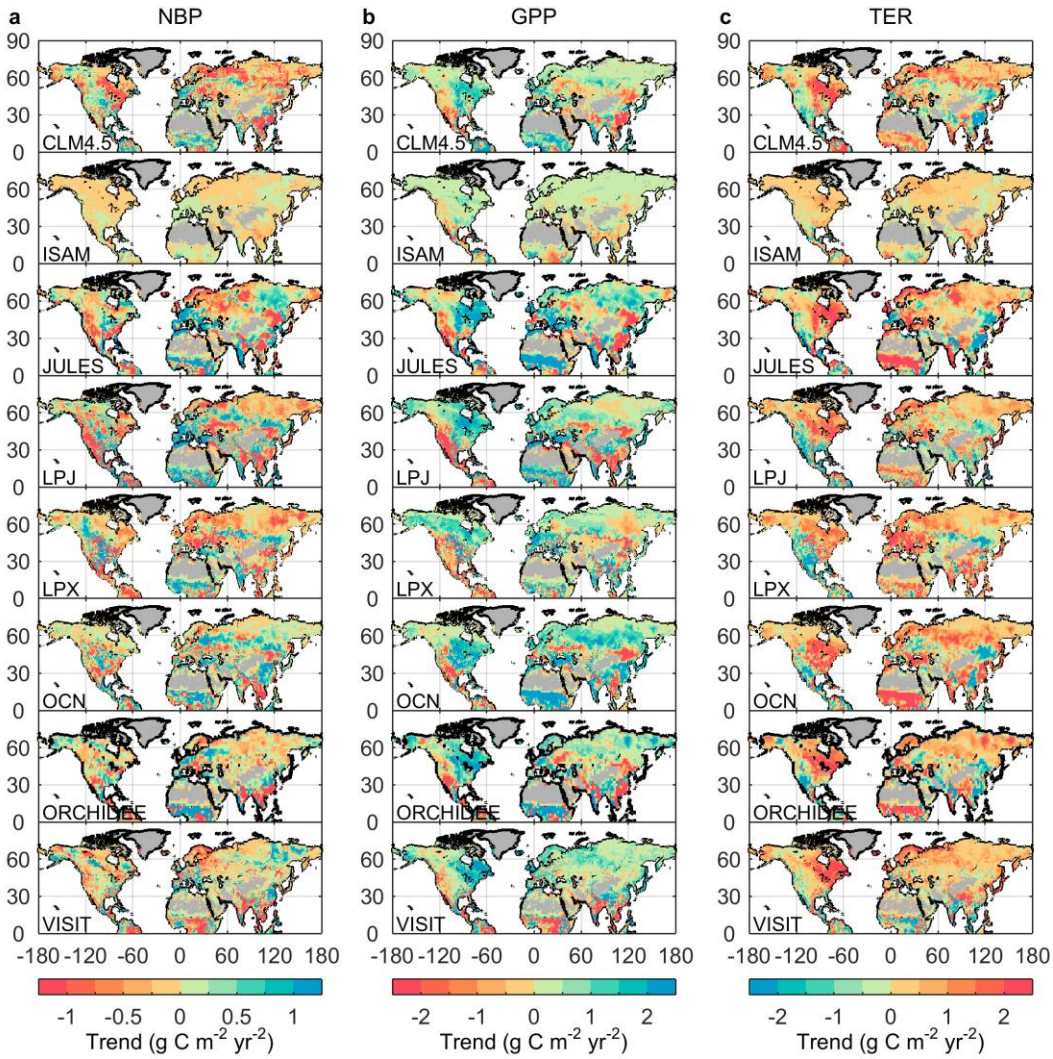

Figure S12 Same as Figure S8, but for trends in CO_2 seasonal trough-to-peak amplitude (AMP_{T-P}).

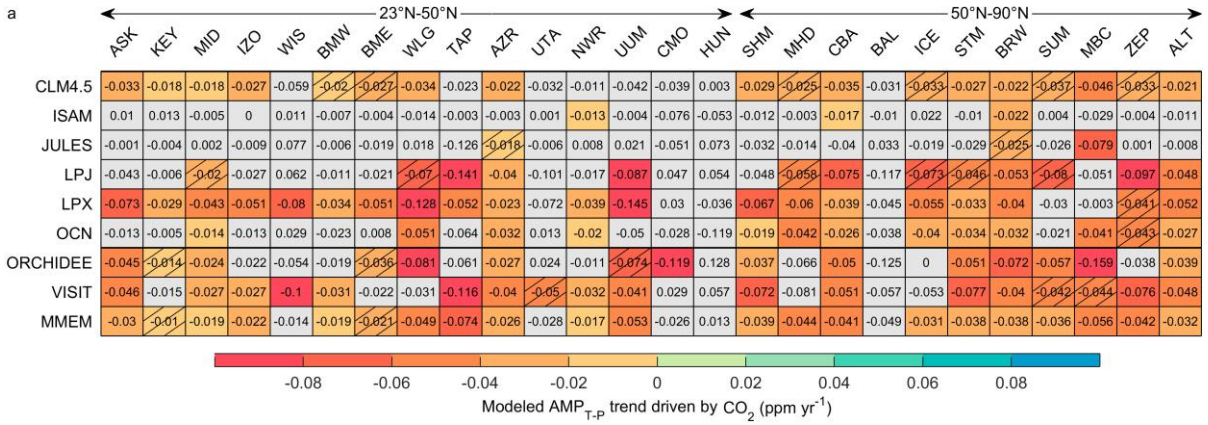

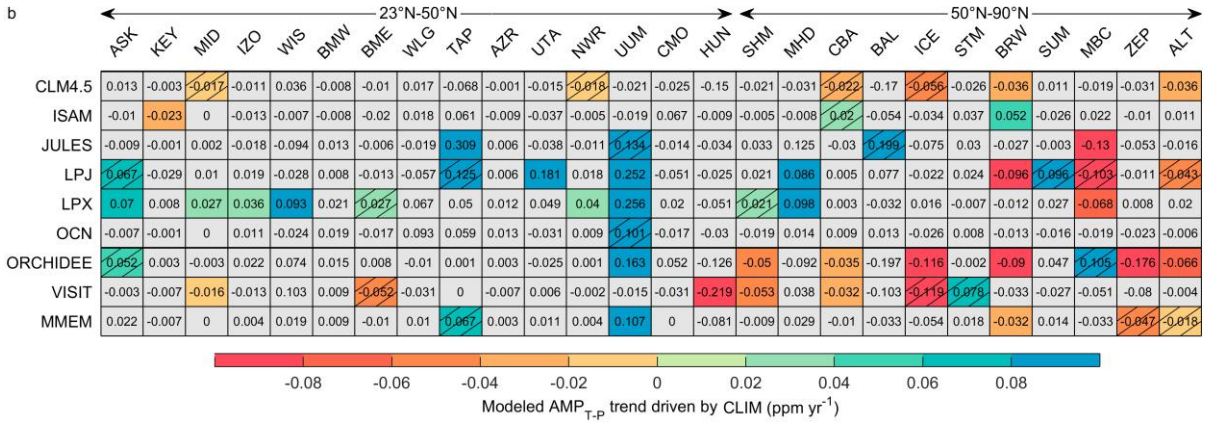

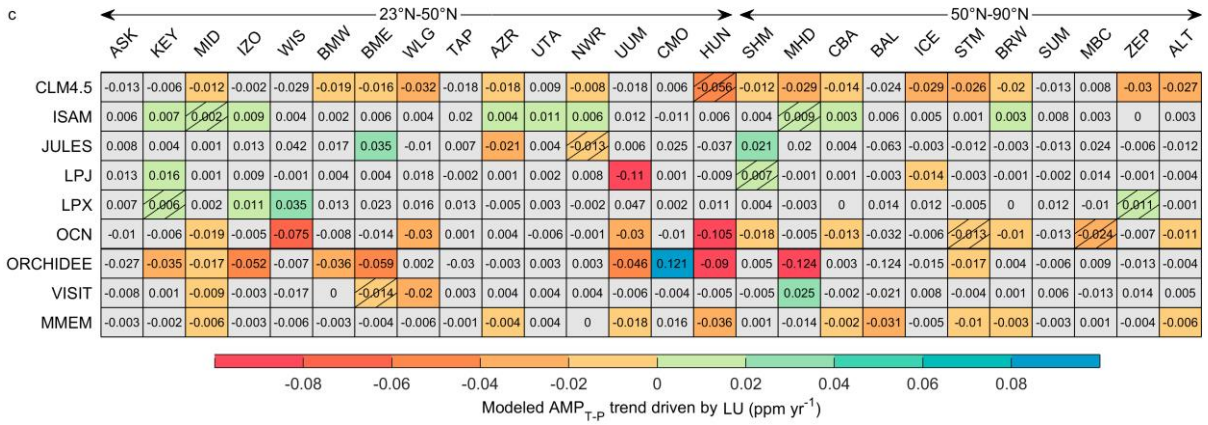

d

	ASK	KEY	MID	IZO	WIS	BMW	BME	WLG	TAP	AZR	UTA	NWR	UUM	CMO	HUN	SHM	MHD	CBA	BAL	ICE	STM	BRW	SUM	MBC	ZEP	ALT
	23°N-50°N															50°N-90°N										
CLM4.5	0.001	0.014	0.005	0.005	0.001	-0.001	0.027	-0.004	0.023	-0.005	0.003	-0.005	0.006	0.02	0.061	0.012	0.004	-0.007	-0.012	0.011	-0.008	0.004	0.007	0.012	0.006	-0.002
ISAM	-0.004	0.012	0.001	0.004	0.012	-0.007	0.001	0.006	0.071	-0.002	0.019	-0.008	-0.006	-0.025	-0.087	0.005	0.04	0.01	-0.018	0.009	-0.004	0.019	-0.014	-0.003	-0.014	-0.003
JULES	-0.009	0.029	0.012	-0.001	0.038	-0.014	0.049	0.014	0.066	-0.026	0.028	0.005	0	0.046	-0.038	-0.013	-0.09	-0.014	-0.007	-0.044	-0.003	0.017	-0.015	0.053	-0.032	-0.013
LPJ	0.002	0.036	0	0.003	0.039	0.016	0.021	0.042	-0.023	-0.006	0.191	0.018	0.015	0.054	0.029	0.013	0.004	-0.045	-0.037	-0.017	-0.005	-0.007	0.012	0.039	-0.028	-0.006
LPX	-0.017	0.003	-0.002	-0.004	0.025	-0.001	0.009	0.025	-0.009	-0.001	-0.025	0	-0.029	0.071	0.041	-0.006	0.008	-0.002	-0.006	-0.003	-0.005	-0.009	0	-0.006	0.007	-0.003
OCN	0.003	0.016	0.001	0.013	-0.024	0.001	0.021	-0.015	0.04	-0.002	0.033	0.009	0.012	-0.007	0.018	-0.004	0.027	0.001	0.012	-0.001	0.008	-0.004	-0.003	-0.008	-0.023	0
ORCHIDEE	0.004	-0.015	-0.002	-0.011	0.05	0.003	-0.015	-0.015	-0.029	0.006	0.082	0.01	-0.005	0.034	0.072	-0.002	0.04	-0.009	-0.073	0.011	0	-0.01	-0.008	-0.013	-0.017	-0.008
VISIT	-0.009	0.017	-0.008	-0.008	-0.015	0.013	-0.019	-0.034	-0.048	-0.003	0.029	-0.008	-0.007	0.029	0.067	-0.032	0.027	-0.003	-0.014	-0.029	0.008	0.003	-0.006	-0.008	-0.001	0.002
MMEM	-0.004	0.014	0.001	0	0.016	0.001	0.012	0.002	0.011	-0.005	0.045	0.003	-0.002	0.028	0.02	-0.003	0.008	-0.009	-0.019	-0.008	-0.001	0.002	-0.004	0.008	-0.013	-0.004

e

	ASK	KEY	MID	IZO	WIS	BMW	BME	WLG	TAP	AZR	UTA	NWR	UUM	CMO	HUN	SHM	MHD	CBA	BAL	ICE	STM	BRW	SUM	MBC	ZEP	ALT
	23°N-50°N															50°N-90°N										
CLM4.5	0.003	0.001	-0.002	0	-0.008	0.002	-0.001	-0.003	0.002	0.003	-0.004	0.001	-0.004	-0.018	0.005	0.004	-0.003	0.005	0.004	-0.006	-0.007	-0.01	0.015	-0.012	-0.003	0
ISAM	0.002	0.001	-0.002	-0.001	-0.007	0.002	0	-0.003	0.004	0.003	-0.004	0	-0.004	-0.018	0.005	0.002	-0.003	0.005	0.004	-0.003	-0.007	-0.01	0.015	-0.012	-0.003	0
JULES	0.003	0.001	-0.002	0	-0.006	0.002	0	-0.003	0.003	0.004	-0.004	0	-0.004	-0.019	0.005	0.004	-0.003	0.006	0.004	-0.004	-0.007	-0.01	0.013	-0.013	-0.003	0
LPJ	0.003	0.001	-0.002	0	-0.007	0.002	0	-0.003	0.003	0.003	-0.004	0.001	-0.004	-0.018	0.005	0.002	-0.003	0.006	0.004	-0.004	-0.007	-0.01	0.014	-0.011	-0.003	0
LPX	0.002	0.001	-0.002	-0.001	-0.007	0.003	-0.001	-0.003	0.003	0.003	-0.004	0.001	-0.004	-0.019	0.005	0.004	-0.004	0.006	0.004	-0.006	-0.006	-0.01	0.014	-0.011	-0.003	0
OCN	0.003	0.001	-0.002	0	-0.007	0.002	0	-0.003	0.003	0.004	-0.004	0.001	-0.004	-0.019	0.005	0.003	-0.003	0.005	0.005	-0.005	-0.006	-0.01	0.014	-0.012	-0.002	0
ORCHIDEE	0.003	0.001	-0.002	-0.001	-0.007	0.002	-0.001	-0.003	0.003	0.004	-0.004	0.001	-0.004	-0.018	0.005	0.004	-0.004	0.005	0.004	-0.005	-0.007	-0.01	0.015	-0.012	-0.003	0
VISIT	0.002	0.001	-0.003	-0.001	-0.007	0.003	0	-0.003	0.003	0.004	-0.004	0.001	-0.004	-0.018	0.005	0.001	-0.003	0.006	0.004	-0.005	-0.007	-0.01	0.014	-0.012	-0.004	0
MMEM	0.003	0.001	-0.002	0	-0.007	0.002	0	-0.003	0.003	0.003	-0.004	0.001	-0.004	-0.018	0.005	0.003	-0.003	0.006	0.004	-0.005	-0.007	-0.01	0.014	-0.012	-0.003	0

f

	ASK	KEY	MID	IZO	WIS	BMW	BME	WLG	TAP	AZR	UTA	NWR	UUM	CMO	HUN	SHM	MHD	CBA	BAL	ICE	STM	BRW	SUM	MBC	ZEP	ALT
	23°N-50°N															50°N-90°N										
CLM4.5	-0.03	-0.014	0.005	-0.034	-0.027	0.009	-0.056	-0.025	-0.027	0.009	-0.038	0.003	0.115	0.037	-0.108	0.011	0.104	-0.026	0.01	-0.058	0.009	-0.016	-0.029	-0.152	0.047	0.018
ISAM	-0.011	-0.029	-0.015	-0.038	-0.063	-0.01	-0.07	-0.015	-0.118	0.016	-0.041	0.023	0.028	0.003	0.035	-0.025	-0.031	-0.026	0.018	-0.048	0.035	-0.022	0.037	-0.107	0.048	0.024
JULES	0.074	-0.043	-0.022	-0.045	-0.125	-0.028	-0.095	-0.022	-0.099	0.043	-0.023	0.029	-0.015	-0.048	0.073	-0.05	0.064	0.042	0.023	-0.065	0.031	-0.011	0.031	-0.13	0.049	0.033
LPJ	0.039	-0.008	0.004	-0.026	-0.034	0.019	-0.072	-0.109	-0.055	-0.029	-0.167	-0.035	0.08	-0.012	-0.036	0.049	0.039	-0.069	0.09	-0.042	-0.01	-0.021	-0.043	-0.077	0.021	0.006
LPX	-0.029	0.005	0.009	-0.012	0.036	-0.007	0.027	0.014	-0.03	-0.023	-0.038	-0.007	0.068	-0.006	-0.151	0.025	0.001	-0.007	-0.004	-0.026	0.011	-0.004	-0.028	-0.047	-0.003	0
OCN	0.037	-0.003	0.025	-0.017	0.002	0.014	0.029	0.002	-0.125	-0.024	-0.046	-0.004	0.081	0.01	-0.078	0.013	0	-0.019	-0.027	-0.022	-0.003	0.004	-0.011	-0.007	-0.003	0.006
ORCHIDEE	0.043	0.035	0.059	-0.008	0.083	0.044	0.114	0.11	-0.03	-0.078	-0.109	-0.037	0.153	0.144	-0.17	0.118	-0.019	0.016	0.106	-0.04	-0.012	0.004	-0.027	0.154	-0.054	-0.018
VISIT	-0.055	-0.034	0.007	-0.027	-0.016	0.012	-0.029	-0.104	-0.078	-0.003	-0.04	-0.011	0.094	-0.083	-0.106	0.002	0.121	-0.022	-0.017	-0.068	-0.004	-0.01	0.001	-0.052	-0.007	0.004
MMEM	0.008	-0.011	0.009	-0.026	-0.018	0.007	-0.019	-0.019	-0.07	-0.011	-0.063	-0.005	0.075	0.006	-0.067	0.018	0.035	-0.014	0.025	-0.046	0.007	-0.01	-0.008	-0.052	0.012	0.009

Figure S13 Spatial distribution of trends in net biome productivity (NBP) (a), gross primary productivity (GPP) (b) and total ecosystem respiration (TER) (c) from September to March for eight Trendy models driven by rising CO_2 only. Note that the period from September to March corresponds to the carbon release period (CRP) of most northern temperate and boreal stations. Regions with mean annual NDVI (AVHRR NDVI3 g dataset) less than 0.1 were masked. The study period is from 1980 to 2012.

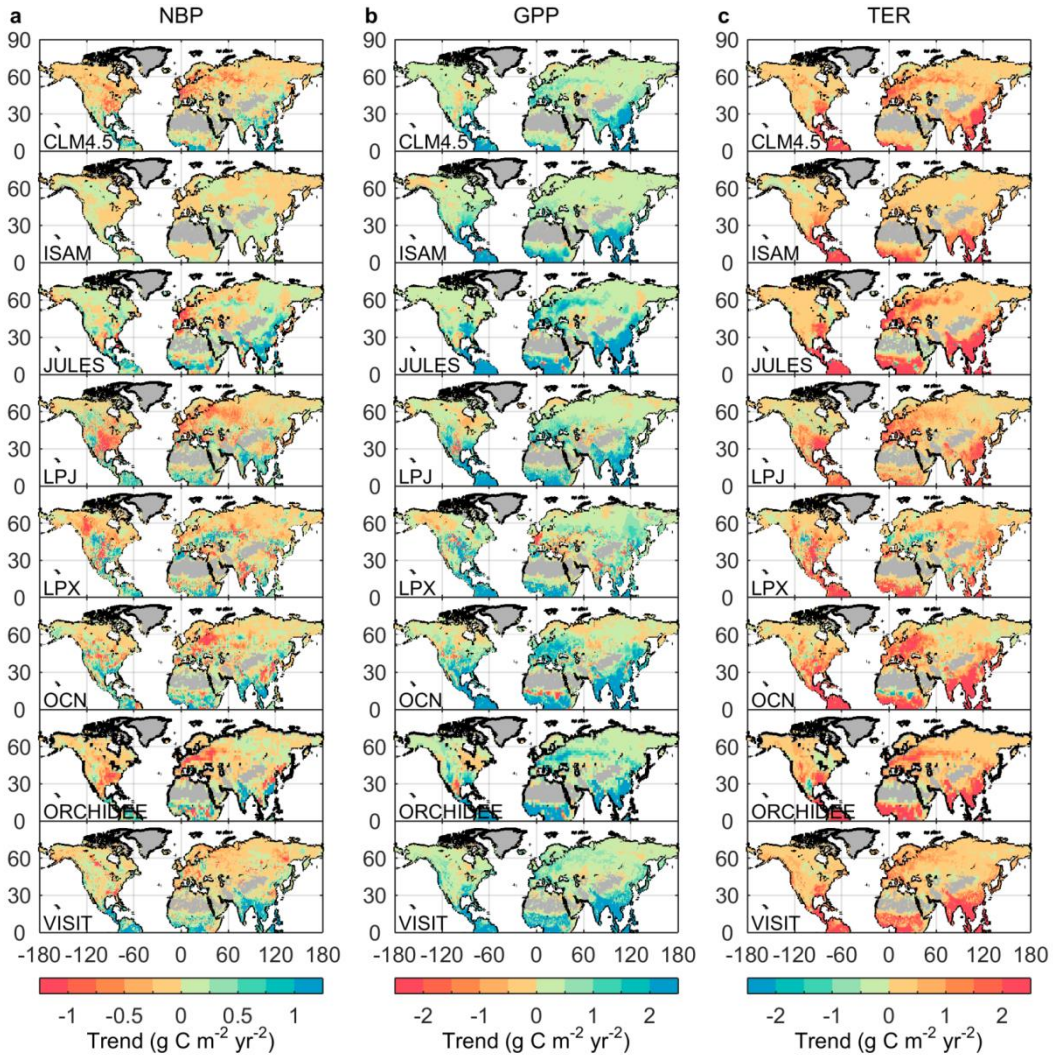

References

Clark, D. B., Mercado, L. M., Sitch, S., Jones, C. D., Gedney, N., Best, M. J., ... & Cox, P. M. (2011). The Joint UK Land Environment Simulator (JULES), model description -Part 2: carbon fluxes and vegetation dynamics. Geoscientific Model Development, **4**, 701-722.

Jain, A. K., Meiyappan, P., Song, Y., & House, J. I. (2013). CO_2 emissions from land-use change affected more by nitrogen cycle, than by the 9 choice of land-cover data. Global Change Biology, **19**, 2893–2906.

Kato, E., Kinoshita, T., Ito, A. & Yamagata, Y. (2013). Evaluation of spatially explicit emission scenario of land-use change and biomass burning using a process-based biogeochemical model. Journal of Land Use Science, **8**, 104-122.

Krinner, G., Viovy, N., de Noblet-Ducoudré, N., Ogée, J., Polcher, J., Friedlingstein, P., ... & Prentice, I.C. (2005). A dynamic global vegetation model for studies of the coupled atmosphere-biosphere system. Global Biogeochemical Cycles, **19**, 1-33.

Oleson, K. W., Lawrence, D.M., Gordon, B., Drewniak, B., Huang, M. Koven, C. D., … & Yang Z. (2013). Technical Description of version 4.5 of the Community Land Model (CLM). NCAR Technical Note NCAR/TN 503+STR; The National Center for Atmospheric Research (NCAR): Boulder, CO.

Sitch, S., Smith, B., Prentice, I. C., Arneth, A., Bondeau, A., Cramer, W., ... & Venevsky, S. (2003). Evaluation of ecosystem dynamics, plant geography and terrestrial carbon cycling in the LPJ dynamic global vegetation model. Global

Change Biology, **9**, 161-185.

Smith, B., Prentice, I. C., & Sykes, M. T. (2001). Representation of vegetation dynamics in the modelling of terrestrial ecosystems: comparing two contrasting approaches within European climate space. Global Ecology and Biogeography, **10**, 621–637.

Stocker, B. D., Roth, R., Joos, F., Spahni, R., Steinacher, M., Zaehle, S., Bouwman, L., & Prentice, I. C. (2013). Multiple greenhouse-gas feedbacks from the land biosphere under future climate change scenarios. Nature Climate Change, **3**, 666-672.

Zaehle, S. & Friend, A. D. (2010). Carbon and nitrogen cycle dynamics in the O-CN land surface model: 1. Model description, site-scale evaluation, and sensitivity to parameter estimates. Global Biogeochemical Cycles, **24**, GB1005.